PHYSICAL REVIEW B VOLUME 35, NUMBER 16 1 JUNE 1987

Site percolation on central-force elastic networks

M. F. Thorpe
Department of Physics and Astronomy, Michigan State University, East Lansing, Michigan 48824

E. J. Garboczi
Armstrong World Industries, Inc., Research and Development, P.O. Box 3511, 2500 Columbia Avenue, Lancaster, Pennsylvania 17604

(Received 30 October 1986)

The elastic properties of model random networks are studied, in which a fraction p_s of the *sites* are randomly present and are connected to their remaining nearest neighbors by Hooke springs with force constant α. The one-site-defect problem is solved exactly using Green's-function techniques specialized to the static elastic limit. The location of p_s^*, the critical point at which all the elastic moduli vanish, and $f(p_s)$, the fraction of zero-frequency modes, agree well with the predictions of constraint-counting theory. In contrast to previously studied *bond*-depletion problems, it is shown both analytically and numerically that Cauchy's relation ($C_{12}=C_{44}$) is strictly *disobeyed*, even in the one-site-defect limit.

I. INTRODUCTION

Our previous work[1-3] on the elastic properties of central-force elastic networks has focused on systems in which various kinds of bonds were distributed according to random *bond-depletion* statistics. Effective-medium theories (EMT) were developed for each of the three cases studied: nearest-neighbor bonds that were missing or present,[1] nearest- and next-nearest-neighbor bonds that were missing or present,[2] and nearest- and next-nearest-neighbor bonds that were strong or weak.[3] In each case, to develop the EMT one first solves the one-defect problem (one changed bond embedded in the network of original bonds), and then uses the probability distribution of the bond strengths to generate the EMT equations for any number of defects. The one-defect problem is easy to solve for these cases, because changing one bond affects only two sites. Some work has also been done to extend EMT to networks which have noncentral forces.[4] The one-defect problem becomes much harder when angular forces are present, because more than two sites are affected.

In this paper we treat the problem of site percolation (site depletion) on networks with nearest-neighbor central forces, the analog of the bond-depletion problem studied in Ref. 1. This case is of interest because the associated single-defect problem is intermediate in difficulty between the central-force and angular force problems. A missing site defect affects many more sites than does a missing bond defect, but the assumption of central forces simplifies much of the work. The site-depletion problem is also of interest because it has a distribution of missing bonds that is qualitatively different from that of a bond-depletion problem. This gives another kind of random central-force network on which to test the validity of Cauchy's relation ($C_{12}=C_{44}$) which has been found to hold, within numerical accuracy, on systems with random *bond* strengths.[1-3]

Section II adapts constraint counting arguments to the site-depletion problem and presents computer simulation results for the fraction of zero frequency modes and elastic moduli of the triangular net and fcc lattice. The solution to the one-site-defect problem is developed in Sec. III. Section IV discusses our numerical and analytical results.

II. NUMERICAL RESULTS

The lattice potential for the networks considered is

$$V=\tfrac{1}{2}\alpha \sum_{\langle i,j\rangle} p_i p_j (l_{ij}-l_0)^2 , \tag{1}$$

where α is the spring force constant, l_{ij} is the strained length of the bond connecting sites i and j and l_0 is its unstrained length, and p_i is a random variable taking on the value 1 if the ith site is present, and 0 otherwise. The angular bracket in (1) restricts the summation to nearest-neighbor pairs. The random variable p_i takes on the value 1 or 0 with probability p_s or $1-p_s$, where p_s is the fraction of *sites* present. It is easy to see that $p=p_s^2$ is the fraction of *bonds* present. In the harmonic limit of small displacements, the lattice potential (1) becomes

$$V=\tfrac{1}{2}\alpha \sum_{\langle i,j\rangle} p_i p_j [(\mathbf{u}_i-\mathbf{u}_j)\cdot\hat{\boldsymbol{\delta}}_{ij}]^2 , \tag{2}$$

where $\mathbf{u}_i$ and $\mathbf{u}_j$ are the displacements from equilibrium of sites i and j, and $\hat{\boldsymbol{\delta}}_{ij}$ is a unit vector from i to j.

We first develop the constraint counting prediction for f, the fraction of zero frequency modes, and then use f to approximately locate p_s^*, the critical value of the site fraction at which the elastic moduli go to zero.

For a network with N sites originally and z nearest neighbors in d dimensions, the total number of constraints N_c will be approximately equal to the total number of bonds present:

$$N_c = \tfrac{1}{2}Nzp = \tfrac{1}{2}Nzp_s^2 \ . \tag{3}$$

Now, when the site is removed, we create d trivial zero-frequency modes that do not affect the rigidity of the remaining network. The fraction of zero-frequency modes f is therefore defined for the *remaining* network and is given by

$$f(p_s) = (dNp_s - \tfrac{1}{2}Nzp_s^2)/dNp_s = 1 - \frac{zp_s}{2d} \ , \tag{4}$$

where dNp_s is the total number of degrees of freedom of the remaining network.

Setting $f(p_s)$ to zero in the usual way[1,2] gives the estimate $p_s^* = 2d/z$ for the rigidity transition[5] point at which the elastic moduli vanish. It is interesting to note that p_s^* is numerically identical to p^*, the constraint counting prediction for bond-depleted networks derived in Ref. 1. However, one must remember that p_s^* refers to the fraction of *sites* present. The corresponding bond fraction would be $p^* = (p_s^*)^2 = 4d^2/z^2$. For the triangular net, $d=2$, $z=6$, so that $p_s^* = \frac{2}{3}$, and for the fcc lattice $d=3$, $z=12$ giving $p_s^* = \frac{1}{2}$.

The insets in Figs. 1 and 2 show $f(p_s)$ for the triangular net and fcc lattice, respectively. The solid lines are the prediction of Eq. (4) and the points are numerical results from a negative eigenvalue algorithm[6] adapted for sparse random matrices. The algorithm finds the number of modes less than a cutoff frequency ω^2 [$\omega^2 \leq 10^{-5}$ in this case in units where the maximum ω^2 is 0(1)]. The triangular net results were obtained using three configurations of a $30\times34=1020$ site net for $p_s > 0.27$, and a $60\times70=4200$ site lattice for $p_s \leq 0.27$. The lattice sizes for the fcc results ranged from 2048 sites (ten configurations) for the smallest values of p_s, to 256 sites (three configurations) for the largest values of p_s. In both figures, good agreement with Eq. (4) is seen except near

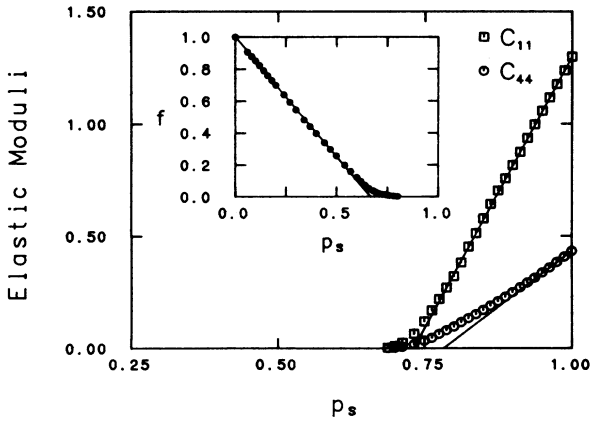

FIG. 1. Showing the two independent elastic moduli C_{11} and C_{44} vs the site fraction p_s for the triangular net. Each data point has been averaged over ten configurations of a 40×46 lattice. The results for C_{11} were also averaged over the x and y directions. The solid lines are the exact initial slopes extrapolated to zero. The inset shows the fraction of zero-frequency modes $f(p_s)$ averaged over the configurations of a 60×70 (30×34) triangular net for $p_s \leq 0.27$ ($p_s > 0.27$). The solid line is the constraint counting result from Eq. (4).

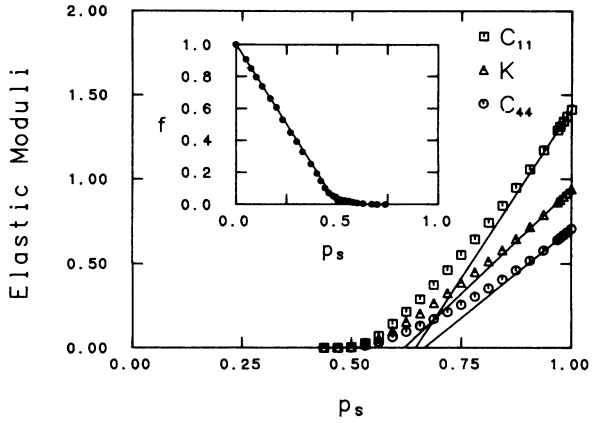

FIG. 2. Showing the three independent elastic moduli C_{11}, K, and C_{44} vs the site fraction p_s for the fcc lattice. Each data point has been averaged over five configurations of an $8\times8\times8$ (2048 site) lattice. C_{11} and C_{44} were also averaged over the x, y, and z directions. The solid lines are the exact initial slopes extrapolated to zero. The inset shows the fraction of zero frequency modes $f(p_s)$ for the fcc lattice. The lattice size and number of configurations averaged over ranged from ten configurations of an $8\times8\times8$ lattice for the smallest values of p_s down to three configurations of a $4\times4\times4$ lattice for the largest p_s values. The solid line is the constraint counting result from Eq. (4).

p_s^*, where the small deviations are due to finite-size numerical effects and overcounting of constraints, since each bond does not represent an independent constraint except as $p_s \to 0$.[4,7]

Figure 1 also shows C_{11} and C_{44} for the triangular net versus the site fraction p_s. The points are an average of ten configurations of a $40\times46=1840$ site cell. C_{11} was also averaged over the x and y directions. The simulations were performed by redefining the shape and/or size of the large unit cell according to the applied strain ϵ. Each site was allowed to relax to its new equilibrium position. The corresponding modulus was then determined from the computed elastic energy per unit volume via the relation $U = \frac{1}{2}C_{ij}\epsilon^2$. The magnitude of ϵ was always of the order 10^{-4}, and periodic boundary conditions were always maintained. An estimate for p_s^* can be obtained from Fig. 1: $p_s^* = 0.71 \pm 0.02$. The constraint counting prediction of $\frac{2}{3}$ differs from this result by about 5%. Chakrabarti, Chowdhury, and Stauffer also found p_s^* to be about $\frac{2}{3}$ in a simulation of a site-depleted triangular network with nearest-neighbor Lennard-Jones forces.[8]

Figure 2 shows C_{11}, K, and C_{44} vs the site fraction p_s for the fcc lattice. The points represent the average of five independent configurations of a 2048-site unit cell ($8\times8\times8$). C_{11} and C_{44} were also averaged over the x, y, and z directions. The simulations were performed in a similar manner to the triangular net simulations. From Fig. 2 we can estimate p_s^* for the fcc lattice to be 0.51 ± 0.02. The constraint counting prediction differs from this result by only 2% and is contained within the error bars.

III. ONE-SITE-DEFECT PROBLEM

When a single site is removed from a network, the effect on the elastic moduli can be solved analytically, which we do in this section. The change in the elastic properties due to a single missing bond is a rather simple problem.[1] The site defect is more complex because the defect matrix is larger. This problem has been previously considered by Lakatos and Krumhansl,[9] although in our case the defect is not as complex and so allows a simpler solution. We will use a technique previously employed by Thorpe and Tang[10] for tight-binding Hamiltonians.

The dynamical matrix[11] for the perfect system in $\mathbf{k}$ space may be written as

$$D_{\alpha\beta}=\alpha\left[\frac{z}{d}\delta_{\alpha\beta}+z\frac{\delta^2\gamma_k}{\delta k_\alpha \delta k_\beta}\right], \tag{5}$$

where

$$\gamma_k=\frac{1}{z}\sum_i e^{ia\mathbf{k}\cdot\hat{\delta}_{0i}} \tag{6}$$

and the sum over i goes over the z nearest neighbors. The unit vector from the origin to one of its nearest neighbors i is $\hat{\delta}_{0i}$. The nearest-neighbor distance is a. The form (5) holds for any Bravais lattice with nearest-neighbor central forces. The equation of motion for the displacements $\mathbf{u}_0$ in the perfect system is

$$m\omega^2\mathbf{u}_0=\vec{\vec{D}}\cdot\mathbf{u}_0 , \tag{7}$$

where $\mathbf{u}_0$ is considered to be a dN vector and $\vec{\vec{D}}$ is the dynamical matrix in real space. It is convenient to work in real space in order to exploit the localized nature of the defect. If an external force $\mathbf{f}_e$, also considered as a dN vector, is applied to the system, then

$$\mathbf{f}_e=-\mathbf{f}=\vec{\vec{D}}\cdot\mathbf{u}_0 . \tag{8}$$

Inverting this equation, we find that

$$\mathbf{u}_0=\vec{\vec{P}}\cdot\mathbf{f} , \tag{9}$$

where $\vec{\vec{P}}$ is the zero-frequency limit of the usual Green function $\vec{\vec{P}}(\omega^2)$ and

$$\vec{\vec{P}}(\omega^2)=(m\omega^2-\vec{\vec{D}})^{-1} . \tag{10}$$

If a single defect is introduced into the system described by (7), then $\vec{\vec{D}}\rightarrow\vec{\vec{D}}+\vec{\vec{V}}$ is a potential localized around the defect. We have the usual Dyson equation

$$\vec{\vec{G}}=\vec{\vec{P}}+\vec{\vec{P}}\,\vec{\vec{V}}\,\vec{\vec{G}} . \tag{11}$$

Here $\vec{\vec{G}}$ is the zero-frequency limit of the Green function $\vec{\vec{G}}(\omega^2)$ for the system including the defect, defined by

$$\vec{\vec{G}}(\omega^2)=(m\omega^2-\vec{\vec{D}}-\vec{\vec{V}})^{-1} . \tag{12}$$

We also set the mass of the defect equal to m, as it is irrelevant for the elastic moduli in the static limit. It simplifies the notation a little to have all the masses equal. The formal solution of (11) is

$$\vec{\vec{G}}=(1-\vec{\vec{P}}\,\vec{\vec{V}})^{-1}\vec{\vec{P}} . \tag{13}$$

The static energy of the system including the defect is

$$E=\tfrac{1}{2}\mathbf{f}_e\cdot\mathbf{u} . \tag{14}$$

Thus, the change in the energy due to the introduction of a defect is

$$\Delta E=-\tfrac{1}{2}\mathbf{f}\cdot\vec{\vec{G}}\cdot\mathbf{f}+\tfrac{1}{2}\mathbf{f}\cdot\vec{\vec{P}}\cdot\mathbf{f}_e , \tag{15}$$

where we have used (9) and also a similar equation with $\vec{\vec{P}}$, $\mathbf{u}_0$ replaced by $\vec{\vec{G}}$, $\mathbf{u}$ when the defect is introduced. Equation (15) can be conveniently rewritten as

$$\begin{aligned}\Delta E&=-\tfrac{1}{2}\mathbf{f}\cdot(\vec{\vec{G}}-\vec{\vec{P}})\cdot\mathbf{f}\\&=-\tfrac{1}{2}\mathbf{f}\cdot\vec{\vec{P}}\cdot\vec{\vec{V}}\cdot\vec{\vec{G}}\cdot\mathbf{f}\\&=-\tfrac{1}{2}\mathbf{f}\cdot\vec{\vec{P}}\cdot\vec{\vec{V}}(1-\vec{\vec{P}}\,\vec{\vec{V}})^{-1}P\cdot\mathbf{f} \qquad (16a)\\&=-\tfrac{1}{2}\mathbf{u}_0\cdot\vec{\vec{V}}(1-\vec{\vec{P}}\,\vec{\vec{V}})^{-1}\cdot\mathbf{u}_0 . \qquad (16b)\end{aligned}$$

The form (16a) is quite convenient, as the applied force $\mathbf{f}$ is usually only nonzero at the surface. However, (16b) is often more useful in practice and can be rewritten in terms of the familiar $\vec{\vec{T}}$ matrix[12]

$$\vec{\vec{T}}=\vec{\vec{V}}(1-\vec{\vec{P}}\,\vec{\vec{V}})^{-1} \tag{17}$$

so that

$$\Delta E=-\tfrac{1}{2}\mathbf{u}_0\cdot\vec{\vec{T}}\cdot\mathbf{u}_0 . \tag{18}$$

This is a convenient form for developing effective-medium theories of many defects as well as the single defect problem we are considering here. Equation (18) is simple because the range of $\vec{\vec{T}}$ is the same as $\vec{\vec{V}}$ and so is localized around the defect. To calculate ΔE, it is therefore necessary to know $\mathbf{u}_0$ only around the defect. Remember that the $\mathbf{u}_0$ are the displacements produced by the external force $\mathbf{f}_e$ in the *absence* of the defect. The situation is particularly simple in a Bravais lattice if $\mathbf{f}_e$ is a uniform external stress (e.g., shear, compression). Then the lattice is uniformly distorted and the $\mathbf{u}_0$ are easy to write down. This is the only case considered here.

Consider a uniform homogeneous distortion of the perfect crystal in which the displacement of the ith atom is

$$\mathbf{u}_i=\epsilon(\mathbf{R}_i\cdot\hat{\boldsymbol{\alpha}})\hat{\boldsymbol{\beta}} , \tag{19}$$

where ϵ is the magnitude of the strain and $\hat{\boldsymbol{\alpha}}$ and $\hat{\boldsymbol{\beta}}$ are Cartesian unit vectors. The vector $\mathbf{R}_i$ is the equilibrium position of the ith atom. The elastic energy associated with (19) for the potential (2) is

$$E=\tfrac{1}{2}\alpha a^2\sum_{\langle i,j\rangle}[(\hat{\delta}_{ij}\cdot\hat{\boldsymbol{\alpha}})(\hat{\delta}_{ij}\cdot\hat{\boldsymbol{\beta}})]^2\epsilon^2 , \tag{20}$$

where $\hat{\delta}_{ij}=\mathbf{R}_{ij}/a$ is a unit nearest-neighbor vector and a is the nearest-neighbor distance. Hence we can write

$$E=\tfrac{1}{4}Nz\epsilon^2a^2\alpha\langle(\delta^\alpha)^2(\delta^\beta)^2\rangle , \tag{21}$$

where the average $\langle\ \rangle$ goes over the z nearest neighbors of the defect site. Because of the central forces, we need only the components of the distortion (19) in the radial direction on the shell around the defect. It is convenient to put the origin at the defect site. Putting it elsewhere corresponds to a uniform translation and does not affect

the result. We therefore form $\mathbf{u}_0$ from the components $\epsilon(\mathbf{R}_i\cdot\hat{\boldsymbol{\alpha}})(\mathbf{R}_i\cdot\hat{\boldsymbol{\beta}})$ on the shell. We set $\mathbf{R}_i=\mathbf{R}_{0i}$ and $\hat{\boldsymbol{\delta}}_i=\hat{\boldsymbol{\delta}}_{0i}$. The normalization of $\mathbf{u}_0$ is given by

$$\epsilon^2\sum_i(\mathbf{R}_i\cdot\hat{\boldsymbol{\alpha}})^2(\mathbf{R}_i\cdot\hat{\boldsymbol{\beta}})^2=\epsilon^2a^2a\langle(\delta^\alpha)^2(\delta^\beta)^2\rangle\ . \tag{22}$$

Therefore, we may write

$$\mathbf{u}_0=\epsilon a[z\langle(\delta^\alpha)^2(\delta^\beta)^2\rangle]^{1/2}\,|\,s\rangle\ , \tag{23}$$

where $|\,s\rangle$ is a unit state vector. Thus, the change in the energy volume for a single defect may be written as

$$\Delta E=-\tfrac{1}{2}z\epsilon^2a^2\langle(\delta^\alpha)^2(\delta^\beta)^2\rangle\langle s\,|\,\vec{\vec{\mathbf{T}}}\,|\,s\rangle\ . \tag{24}$$

Remembering that when the defect is introduced, the *stress* is held constant, so that it is the quantity α^{-1} that is renormalized as the energy $\sim f^2/\alpha$. Hence we may write

$$\frac{\alpha}{\alpha_e}=1+\frac{\mathbf{f}\vec{\vec{\mathbf{P}}}\vec{\vec{\mathbf{T}}}\vec{\vec{\mathbf{P}}}\mathbf{f}}{\mathbf{f}\vec{\vec{\mathbf{P}}}\mathbf{f}} \tag{25}$$

using Eqs. (13)–(15), where α_e is the renormalized spring force constant. This can be rewritten in terms of the $\mathbf{u}_0$ produced by the $\mathbf{f}$

$$\frac{\alpha}{\alpha_e}=1-\frac{\mathbf{u}_0\vec{\vec{\mathbf{T}}}\mathbf{u}_0}{\mathbf{u}_0\vec{\vec{\mathbf{D}}}\mathbf{u}_0} \tag{26}$$

which is also given by

$$\frac{\alpha}{\alpha_e}=1+\frac{\Delta E}{E}\ . \tag{27}$$

The results (25)–(27) are quite general.[10] In the present case, using (21) and (24), we find that

$$\frac{\alpha}{\alpha_e}=1-\frac{2Nc\langle s\,|\,\vec{\vec{\mathbf{T}}}\,|\,s\rangle}{N\alpha}\ , \tag{28}$$

$$\frac{\alpha}{\alpha_e}=1-2c\langle s\,|\,\vec{\vec{\mathbf{T}}}\,|\,s\rangle/\alpha\ , \tag{29}$$

where Nc is the (small) number of noninteracting defects. It is more usual to invert (29) to give

$$\alpha_e=\alpha+2c\langle s\,|\,\vec{\vec{\mathbf{T}}}\,|\,s\rangle \tag{30}$$

to first order in the concentration c of defects.

If the defect is such that the z bonds around the defect site are α_0 rather than α, then it is easy to see that for any $|\,s\rangle$ formed as above

$$V\,|\,s\rangle=(\alpha_0-\alpha)\,|\,s\rangle \tag{31}$$

and

$$\alpha_e=\alpha+\frac{2c(\alpha_0-\alpha)}{1-(\alpha_0-\alpha)\langle s\,|\,\vec{\vec{\mathbf{P}}}\,|\,s\rangle}\ , \tag{32}$$

where we use the fact that for *certain special strains* $|\,s\rangle$ is an eigenstate of the matrix $\vec{\vec{\mathbf{P}}}$. In the tight-binding model, this is achieved automatically,[10] but here we have to find the appropriate strains. There are exactly the right number of independent eigenstates $|\,s\rangle$ to give a complete solution to the problem. If we write[10]

$$p_I=\frac{1}{2}-\frac{\alpha}{z}\langle s\,|\,\vec{\vec{\mathbf{P}}}\,|\,s\rangle \tag{33}$$

then

$$\alpha_e=\alpha+\frac{2c\alpha(\alpha_0-\alpha)}{2\alpha(1-p_I)+\alpha_0(2p_I-1)} \tag{34}$$

and so for the special case of most interest here, a vacancy where $\alpha_0=0$,

$$\alpha_e=\alpha-\frac{c\alpha}{1-p_I} \tag{35}$$

which gives the initial slope for small c. If this slope is extrapolated to the point at which it crosses the horizontal axis, this occurs at $p=1-c=p_I$; hence the notation.

The quantity p_I is a pure number, and it allows the general site-defect problem (34) to be solved, as well as the vacancy (35). We will now calculate p_I for various strains in the triangular net and fcc lattice.

For the triangular net, the elements of the dynamical matrix in k space may be obtained from γ_k [see Eqs. (5) and (6)]:

$$\gamma_k=\tfrac{1}{6}[2\cos(2x)+4\cos x\cos y]\ , \tag{36}$$

where the x axis is along one of the bonds and we use the shorthand notation $x=k_xa/2$, $y=\sqrt{3}k_ya/2$. Using (5), we see that

$$\begin{aligned}D_{xx}&=3-2\cos(2x)-\cos x\cos y\ ,\\ D_{yy}&=3(1-\cos x\cos y)\ ,\\ D_{xy}&=D_{yx}=\sqrt{3}\sin x\sin y\ .\end{aligned} \tag{37}$$

The group of the site defect in the triangular net is C_{6v} and the radial displacements on the shell around the defect transform[13] as $\Gamma_1+\Gamma_3+\Gamma_5+\Gamma_6$. A second rank tensor transforms as (x^2+y^2) which is Γ_1 and (xy) which is Γ_6. Thus Γ_1 leads to the bulk modulus K and Γ_6 leads to the shear modulus C_{44}. These are the $|\,s\rangle$ that are the eigenstates of P and from these two elastic moduli, all others may be found. The inverse of the dynamical matrix $\vec{\vec{\mathbf{D}}}(\mathbf{k})$ may be written $\vec{\vec{\Lambda}}$ where

$$\begin{aligned}\Lambda_{xx}&=D_{yy}/(D_{xx}D_{yy}-D_{xy}^2)\ ,\\ \Lambda_{yy}&=D_{xx}/(D_{xx}D_{yy}-D_{xy}^2)\ ,\\ \Lambda_{xy}&=\Lambda_{yx}=-D_{xy}/(D_{xx}D_{yy}-D_{xy}^2)\ .\end{aligned} \tag{38}$$

Thus the components of the Green function are

$$P_{ij}^{\alpha\beta}=\frac{1}{N}\sum_{\mathbf{k}}\Lambda_{\alpha\beta}e^{i\mathbf{k}\cdot(\mathbf{R}_i-\mathbf{R}_j)}\ , \tag{39}$$

where i,j denote either the defect atom or an atom on the nearest-neighbor shell.

For the bulk modulus K, we have $\mathbf{u}_i=\epsilon a\hat{\boldsymbol{\delta}}_i$, so after forming the normalized $|\,s\rangle$ state vector as described earlier, we find that

$$p_I=\tfrac{1}{2}-3\sum_{i,j,\alpha,\beta}\delta_i^\alpha P_{ij}^{\alpha\beta}\delta_j^\beta e^{ia\mathbf{k}\cdot(\hat{\boldsymbol{\delta}}_i-\hat{\boldsymbol{\delta}}_j)}\ ,$$

where the sum over i,j goes over the atoms in the shell or

$$p_I = \frac{1}{2} - \frac{3}{N} \sum_{\mathbf{k},\alpha,\beta} \frac{\delta\gamma_k}{\delta\alpha} \Lambda_{\alpha\beta} \frac{\delta\gamma_k}{\delta\beta} , \tag{40}$$

where

$$\frac{\delta\gamma_k}{\delta x} = -\tfrac{1}{3}[\sin(2x) + \sin x \cos y]$$

and

$$\frac{\delta\gamma_k}{\delta y} = -\frac{1}{\sqrt{3}} \cos x \sin y .$$

For the shear modulus C_{44}, we project into the radial direction to get $\mathbf{u}_i = \epsilon a(\hat{\boldsymbol{\delta}}_i \cdot \hat{\mathbf{x}})(\hat{\boldsymbol{\delta}}_i \cdot \hat{\mathbf{y}})\hat{\boldsymbol{\delta}}_i$. After forming the state vector $|s\rangle$ we find that

$$p_I = \tfrac{1}{2} - \tfrac{2}{3} \sum_{i,j,\alpha,\beta} \delta_i^x \delta_i^y \delta_i^\alpha P_{ij}^{\alpha\beta} \delta_j^\beta \delta_j^x \delta_j^y e^{ia\mathbf{k}\cdot(\hat{\delta}_i - \hat{\delta}_j)}$$

$$= \frac{1}{2} - \frac{24}{N} \sum_{k,\alpha,\beta} \frac{\delta^3\gamma_k}{\delta x \delta y \delta\alpha} \Lambda_{\alpha\beta} \frac{\delta^3\gamma_k}{\delta x \delta y \delta\beta} . \tag{41}$$

Evaluating the factors involving the derivatives of γ_k, we find

$$\frac{\delta^3\gamma_k}{\delta x \delta y^2} = \tfrac{1}{4} \sin x \cos y ,$$
$$\frac{\delta^3\gamma_k}{\delta x^2 \delta y} = \frac{1}{4\sqrt{3}} \cos x \sin y . \tag{42}$$

The integrals (40) and (41) are over the first Brillouin zone and can be evaluated numerically. The values are given in Table I. From these two, the p_I for all other elastic moduli can be found. Some of these are also shown in Table I.

For the fcc lattice, the calculation proceeds similarly to the case of the triangular net, so we give only the essential steps. The elements of the dynamical matrix may be obtained from γ_k:

$$\gamma_k = \tfrac{1}{3}(\cos x \cos y + \cos y \cos z + \cos z \cos x) , \tag{43}$$

where x, y, and z are the usual cubic axes, and we use the shorthand notation $k_x a/\sqrt{2} = x$, etc. Using (5) we see that

$$D_{xx} = 4 - 2\cos x(\cos y + \cos z) ,$$
$$D_{xy} = 2 \sin x \sin y , \tag{44}$$

plus cyclic permutations to get the other $D_{\alpha\beta}$.

The group of the site defect in the fcc lattice is O_h, and the radial displacements on the shell around the defect transform as $\Gamma_1^+ + \Gamma_1^- + \Gamma_3^+ + \Gamma_4^- + \Gamma_5^+ + \Gamma_5^-$. A second-rank tensor transforms[13] as $(x^2+y^2+z^2)$ which is Γ_1^+, $(x^2-y^2, 3z^2-r^2)$ which is Γ_3^+, and (xy, yz, zx) which is Γ_5^+. Thus Γ_1^+ leads to the bulk modulus K, and Γ_3^+ is the shear modulus $\frac{1}{2}(C_{11}-C_{12})$. This corresponds to a shear along $[1\bar{1}0]$ in the [110] direction, for example. Also Γ_5^+ leads to C_{44} which is a shear along [100] in the [010] direction, for example. These are the $|s\rangle$ that are the eigenstates of P; from these three elastic moduli, all others can be found. It is perhaps surprising that one is led to $\frac{1}{2}(C_{11}-C_{12})$ rather than, say, C_{11}; but that is the way it works out.

Proceeding as in the triangular net, we find the p_I for the bulk modulus K to be

$$p_I = \frac{1}{2} - \frac{6}{N} \sum_{\mathbf{k},\alpha,\beta} \frac{\delta\gamma_k}{\delta\alpha} \Lambda_{\alpha\beta} \frac{\delta\gamma_k}{\delta\beta} \tag{45}$$

for the shear modulus $\frac{1}{2}(C_{11}-C_{12})$

$$p_I = \frac{1}{2} - \frac{36}{N} \sum_{\mathbf{k},\alpha,\beta} \left(\frac{\delta^3\gamma_k}{\delta^2 x \delta\alpha} - \frac{\delta^3\gamma_k}{\delta^2 y \delta\alpha} \right) \times \Lambda_{\alpha\beta} \left(\frac{\delta^3\gamma_k}{\delta^2 x \delta\beta} - \frac{\delta^3\gamma_k}{\delta^2 y \delta\beta} \right) \tag{46}$$

and for the shear modulus C_{44}

$$p_I = \frac{1}{2} - \frac{72}{N} \sum_{\mathbf{k},\alpha,\beta} \frac{\delta^3\gamma_k}{\delta x \delta y \delta\alpha} \Lambda_{\alpha\beta} \frac{\delta^3\gamma_k}{\delta x \delta y \delta\beta} . \tag{47}$$

These expressions are three-dimensional integrals over the first Brillouin zone and are evaluated numerically. The results are shown in Table II. From these three intercepts, the p_I for all other elastic moduli can be found. Some of these are also shown in Table II.

IV. DISCUSSION

In this paper, we have presented numerical simulations and exact analytical initial slope results for the elastic properties of two- and three-dimensional site-depleted central-force networks. Upon comparison with our previous results[1-3] (Ref. 1 in particular) for bond-depleted networks, several interesting similarities and differences may be seen.

TABLE I. List of values of intercepts derived from initial slope calculation for triangular net, in terms of site fraction p_s. Results labeled "Simulation" were obtained by direct numerical simulation of a 40×46 lattice with *one* site missing. Only two of the intercepts are independent.

Modulus	Theory	Simulation
C_{44}	0.782	0.782
K	0.696	0.695
E	0.759	0.759
C_{12}	0.495	0.497
C_{11}	0.731	0.731

TABLE II. List of values of intercepts derived from initial slope calculation for fcc lattice in terms of site fraction p_s. Results labeled "Simulation" were obtained by direct numerical simulation of an $8\times8\times8$ lattice with *one* site missing. Only three of the intercepts are independent.

Modulus	Theory	Simulation
K	0.620	0.620
C_{44}	0.666	0.666
$\frac{1}{2}(C_{11}-C_{12})$	0.688	0.687
C_{12}	0.591	0.591
C_{11}	0.646	0.646

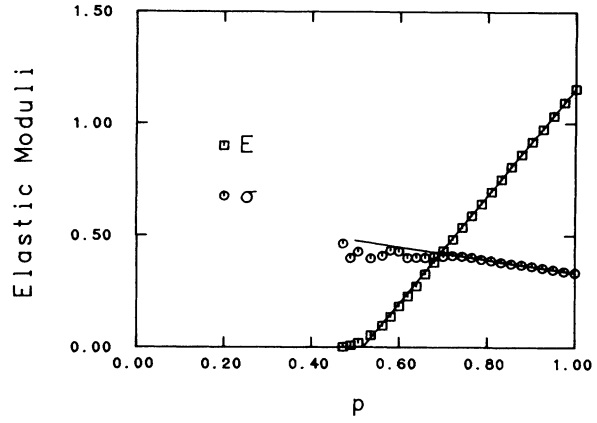

FIG. 3. Showing the Young's modulus E and Poisson's ratio σ vs the *bond* fraction $p=p_s^2$ for the triangular net. The solid lines are the extrapolated exact initial slopes.

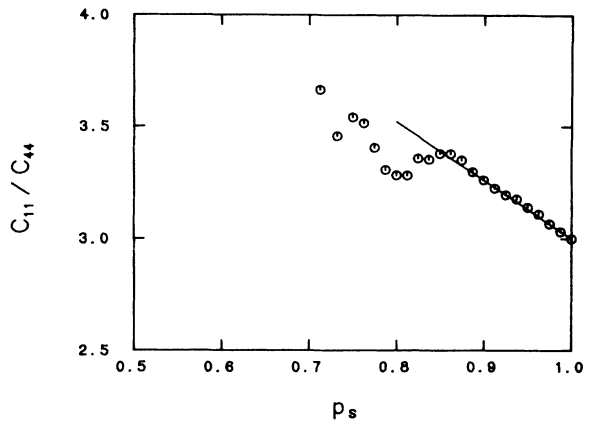

FIG. 5. Showing the ratio C_{11}/C_{44} vs the site fraction p_s for the triangular net. The solid line is the extrapolated exact initial slope.

Simple constraint-counting theory (albeit in a slightly modified form) continues to be a powerful method of locating the rigidity transition[5] point to within a percent or so. The reason for this success is still not clear, as it is known that $f(p_s)$ [or $f(p)$] is *not* equal to zero at the rigidity transition point, since small floppy inclusions persist in the rigid backbone for $p_s > p_s^*$, resulting in the coexistence of zero-frequency modes and finite macroscopic elastic stiffness. It should be noted here that the power of constraint counting also extends to problems with angular forces.[14] The form of $f(p_s)$ was also predicted quite well by constraint counting, except in the critical region around p_s^*.

Figure 3 shows the elastic moduli for the triangular net, in this case the Young's modulus E and the Poisson's ratio σ plotted versus the *bond* fraction p (these quantities can be calculated from the c_{ij} as shown in Ref. 7). The critical point[15] becomes $p^* \cong (0.71)^2 \cong 0.5$. The solid lines are the exact initial slopes replotted versus p. It is easy to show if p_I is the intercept in terms of the site fraction p_s, then $p_I' = 2p_I - 1$ is the intercept in terms of the bond fraction p. The data points for E follow the initial slope remarkably closely. The agreement is nearly as good as in the bond percolation case.[1] Poisson's ratio follows the initial slope well until about $p=0.7$. There is typically more noise in a computed ratio as we are dividing smaller and smaller numbers as $p \to p^*$. Figure 4 is the equivalent of Fig. 3 but for the fcc lattice, showing C_{11}, K, and C_{44} versus p. Again the data points follow the initial slope result quite well. However, the agreement was somewhat better in the bond problem on the fcc lattice.[1] One should note that $p^* = (0.51)^2 = 0.26$.

The elastic behavior of the site-depleted networks differed significantly from that of the analogous bond-depleted networks in the behavior of the ratios of the elastic moduli. In the bond case,[1] the ratios were essentially constant as a function of p, since the agreement with effective medium theory was so good and p_I was the same for all moduli. Figures 5 and 6 show the elastic moduli

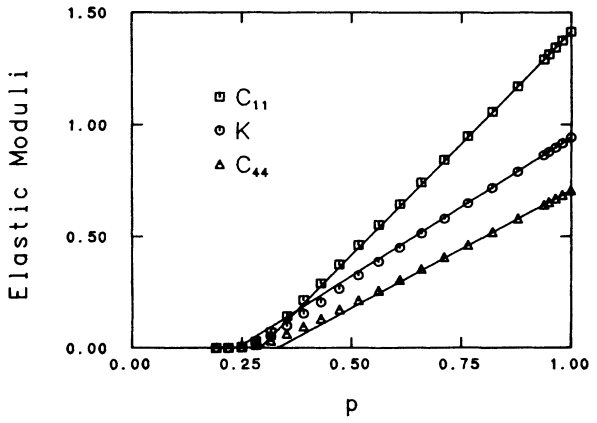

FIG. 4. Showing the elastic moduli C_{11}, K, and C_{44} vs the *bond* fraction $p=p_s^2$ for the fcc lattice. The solid lines are the extrapolated exact initial slopes.

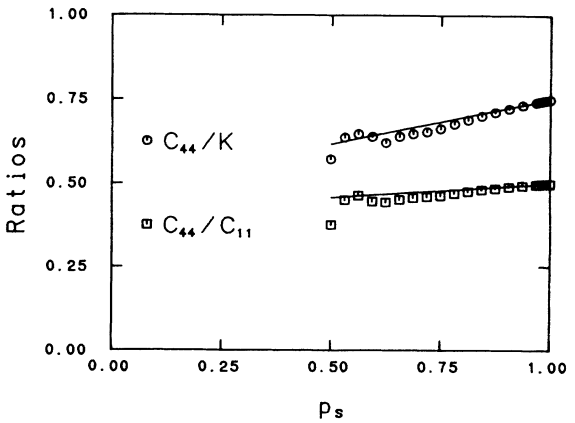

FIG. 6. Showing the ratios C_{44}/K and C_{44}/C_{11} vs the site fraction p_s for the fcc lattice. The solid lines are the extrapolated exact initial slopes

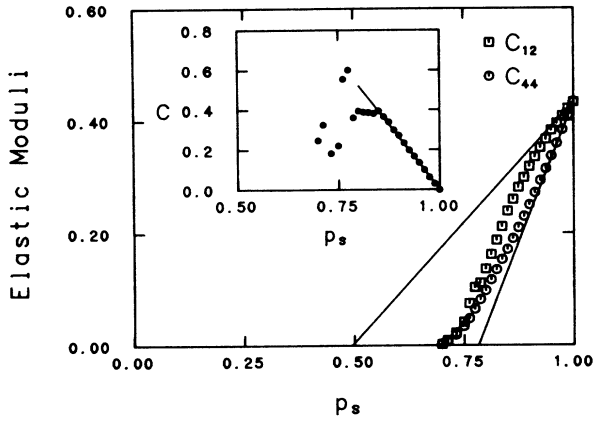

FIG. 7. Showing the elastic moduli C_{12} and C_{44} vs the site fraction p_s for the triangular net. The solid lines are the exact initial slopes extrapolated down to zero. The inset shows C vs p_s, where $C=(C_{12}-C_{44})/C_{44}$. The straight line is the extrapolated exact initial slope.

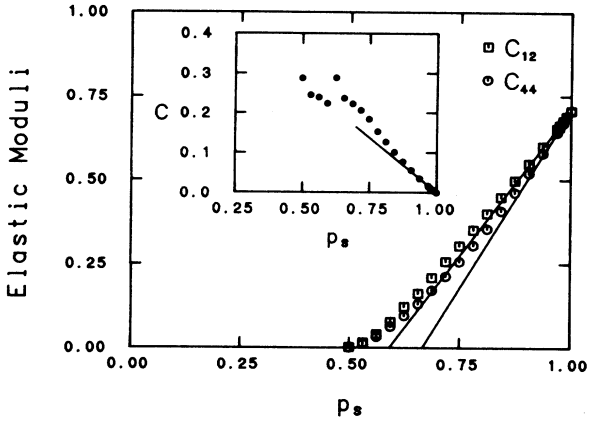

FIG. 8. Showing the elastic moduli C_{12} and C_{44} vs the site fraction p_s for the fcc lattice. The solid lines are the exact initial slopes extrapolated down to zero. The inset shows C vs p_s, where $C=(C_{12}-C_{44})/C_{44}$. The straight line is the extrapolated exact initial slope.

ratios for the site case. C_{11}/C_{44} is plotted in Fig. 5 for the triangular net versus the site fraction p_s. The initial slope of the ratio is non-zero because the initial slopes for C_{11} and C_{44} are different. It is interesting to note that the critical value of the C_{11}/C_{44} ratio is roughly 3.5 ± 0.3, which is the same value Bergman[16] found for C_{11}/C_{44} for the bond-percolation problem on the honeycomb net with angular forces. The reason, if any, for this numerical coincidence is not obvious, as the two problems are in different universality classes.[17] The fcc ratios in Fig. 6 are also not constant.

A more important distinction can be drawn between the central-force site-depletion and bond-depletion elastic problems on the basis of Cauchy's relation. The derivation of Cauchy's relation, as usually stated,[18] states that a network with a center of symmetry at *every* site and only central forces will have $C_{12}=C_{44}$. In the bond-depleted systems, it was found that $C_{12}=C_{44}$ was obeyed with remarkable accuracy even close to the critical region, where the difficulty of relaxing the networks caused large numerical uncertainties. More importantly, however, was that the effective-medium theory in the bond case, which gave the initial slope *exactly*, implied that Cauchy's relation was obeyed exactly even in the presence of a few altered bonds. In the site-depletion case studied here, it was found that the initial slopes of C_{12} and C_{44} were rigorously not the same (see Tables I and II), implying that Cauchy's relation is not obeyed even when only one site defect is present.

C_{12} and C_{44} are plotted versus p_s for the triangular net and fcc lattice in Figs. 7 and 8, respectively. The insets show the parameter $C\equiv(C_{12}-C_{44})/C_{44}$ graphed versus p_s. The solid lines are the extrapolated exact initial slopes. It is clear in both figures that Cauchy's relation is no longer obeyed when site defects are present in a central-force network. The evidence from the bond-depletion studies (Refs. 1–3) already shows that the usual assumptions behind Cauchy's relation may have to be generalized; the negative result in the site-depletion case puts limits on how general such assumptions may be. A possible generalized hypothesis for Cauchy's relation has been proposed and is presented elsewhere along with supporting numerical evidence.[19]

ACKNOWLEDGMENT

The work at Michigan State University is supported by the National Science Foundation under Grant No. DMR 8317610.

[1]S. Feng, M. F. Thorpe, and E. J. Garboczi, Phys. Rev. B **31**, 276 (1985).
[2]E. J. Garboczi and M. F. Thorpe, Phys. Rev. B **31**, 7276 (1985).
[3]E. J. Garboczi and M. F. Thorpe, Phys. Rev. B **33**, 3289 (1986).
[4]L. M. Schwartz, S. Feng, M. F. Thorpe, and P. N. Sen, Phys. Rev. B **32**, 4607 (1985).
[5]M. F. Thorpe, J. Non-Cryst. Solids **57**, 355 (1983).
[6]R. J. Bell, Methods Comput. Phys. **15**, 215 (1976); Rep. Prog. Phys. **35**, 1315 (1972); P. Dean, Rev. Mod. Phys. **44**, 127 (1972).
[7]M. F. Thorpe and P. N. Sen, J. Acous. Soc. Am. **77**, 1674 (1985).
[8]B. K. Chakrabarti, D. Chowdhury, and D. Stauffer, Z. Phys. B **62**, 232 (1986).
[9]K. Lakatos and J. A. Krumhansl, Phys. Rev. **175**, 184 (1968); **180**, 729 (1969).
[10]M. F. Thorpe and W. Tang (unpublished).
[11]See, for example, M. Born and K. Huang, *Dynamical Theory of Crystal Lattices* (Clarendon, Oxford, 1966).
[12]See, for example, R. J. Elliott, J. A. Krumhansl, and P. L.

Leath, Rev. Mod. Phys. **46**, 465 (1974).
[13]See, for example, G. F. Koster, J. O. Dimmock, R. G. Wheeler, and H. Statz, *Properties of the Thirty-Two Point Groups* (M. I. T. Press, Cambridge, 1963).
[14]H. He and M. F. Thorpe, Phys. Rev. Lett. **54**, 2107 (1985).
[15]B. P. Watson and P. L. Leath, Phys. Rev. B **9**, 4893 (1974).
[16]D. J. Bergman, Phys. Rev. B **31**, 1696 (1985).
[17]A. R. Day, R. R. Tremblay, and A.-M. S. Tremblay, Phys. Rev. Lett. **56**, 2501 (1986); E. J. Garboczi and M. F. Thorpe, Phys. Rev. B **32**, 4513 (1985).
[18]A. E. H. Love, *A Treatise on the Mathematical Theory of Elasticity*, 4th ed. (Cambridge University Press, Cambridge, England, 1934); M. Born and K. Huang, *Dynamical Theory of Crystal Lattices* (Clarendon, Oxford, 1966); J. H. Weiner, *Statistical Mechanics of Elasticity* (Wiley, New York, 1983).
[19]E. J. Garboczi, Phys. Rev. B (to be published).